



Terrestrial kilometric radiation observed on pre-midnight side of the Earth at 1-2 L-Shell

Mohammed Y. Boudjada¹, Patrick H.M. Galopeau², Sami Sawas³, Valery Denisenko^{4,5}, Konrad Schwingenschuh¹, Helmut Lammer¹, Hans U. Eichelberger¹, Werner Magnes¹, and Bruno Besser¹

¹Space Research Institute, Austrian Academy of Sciences, Graz, Austria

²LATMOS-CNRS, Université Versailles Saint-Quentin-en-Yvelines, Guyancourt, France

³Institute of Communications and Wave Propagation, University of Technology, Graz, Austria

⁴Institute of Computational Modelling, Russian Academy of Sciences, Krasnoyarsk, Russia

⁵Siberian Federal University, Krasnoyarsk, Russia

Correspondence: M.Y. Boudjada (mohammed.boudjada@oeaw.ac.at)

Abstract. The ICE experiment onboard the DEMETER satellite recorded kilometric emissions in the vicinity of the magnetic equatorial plane. Those radiations were observed in the beginning of the year 2010 on the night-side of the Earth and rarely on the day-side. We distinguish two components one appears as a continuum between few kHz and up to 50 kHz and the other one from 50 kHz to 800 kHz. The first component exhibits positive and negative frequency drift rates in the southern and northern hemispheres, at latitudes between 40° and 20°. The second component displays multiple spaced frequency bands. Such bands mainly occur near the magnetic equatorial plane with a particular enhancement of the power level when the satellite latitude is close to the magnetic equatorial plane. We show in this study that both components are linked to the terrestrial non-thermal kilometric radiation. Those two components are the trapped and the escaping terrestrial non-thermal kilometric radiation. Above 150 kHz, we have found that the escaping emissions are mainly extended in frequency in the southern hemisphere and in geomagnetic latitude in the opposite hemisphere. DEMETER low altitude orbits lead to describe the frequency and the time evolution of this terrestrial radiation particularly on the evening sector at L-Shell of about 2. We show the dependence of the power intensity on the emission frequency, and provide a hint on the location of the source region and its relation to the Earth's plasmasphere. It is shown that the so-called 'Christmas-tree' pattern associated to the terrestrial kilometric radiation may be associated to the plume and channel generated in the pre-midnight sector of the plasmasphere.

15

1 Introduction

A variety of radio waves have been detected in the near Earth's space environment in the seventeens. Imp 6 satellite radio measurements have allowed the identification, for a first time, of a weak continuum associated to the Earth's magnetosphere. The continuum power level was found to be below the cosmic noise level at frequencies of about 100 kHz with a low frequency



- of 30 kHz (Brown, 1973) which was considered to be produced by solar wind local plasma frequency. Another continuum component but more intense have been identified at even lower frequencies, between 5 and 20 kHz (Gurnett and Shaw, 1973). This radiation is found to occur at frequencies smaller than the local plasma frequency of the solar wind. Gurnett (1975) showed that these two types of emission belong to a single non-thermal continuum spectrum, one 'trapped' and the other 'escaping'.
- 5 The first component has frequencies lower than about 30 kHz which correspond to the magnetopause plasma frequency, and the second one has frequencies above this limit. Kurth et al. (1981) showed using ISEE 1 satellite quite temporal and spectral differences between both components. The observed differences are interpreted as the effect of the cavity on the 'trapped' component. Also high resolution spectrograms made evident the presence of numerous narrow-band emissions for the 'escaping' component.
- 10 Recent missions like CLUSTER, GEOTAIL, IMAGE and INTERBALL-1 provide new observations of the terrestrial non-thermal continuum. Hashimoto et al. (1999, 2006) reported about a new component at frequencies of 100 to 800 kHz detected when GEOTAIL satellite was at 10 to 30 R_E inside the Earth's plasmasphere. About one hundred events were recorded during the period from 01st Jan. to 31st Dec. 1996. Events were found to occur on the dayside/evening sectors and within about 10° of the magnetic equator. Kuril'chik et al. (2001, 2007) reported events of kilometric continuum recorded by INTERBALL-1
- 15 satellite very close to the Earth (1.6 to 2.4 R_E) with a high spectral resolution (10 kHz and 0.2 sec) at two frequencies 252 kHz and 500 kHz. Authors showed that the 'continuum' emission has a rather impulsive character, and a dependence of the beam widths on the solar activity. The polar orbit of the IMAGE satellite allowed finding that the non-thermal continuum radiation extends from about 29 kHz to about 500 kHz and forming a 'Christmas tree' pattern, nearly symmetric about the magnetic equator (Green and Boardsen, 2006). IMAGE satellite observations showed that the kilometric continuum is confined to a
- 20 narrow latitude range of about 15°. The source region of the kilometric continuum is found in the plasmopause within notch structures co-rotating with the Earth (Green et al., 2004). First CLUSTER non-thermal continuum observations were reported by Décréau et al. (2001). Direction finding technique, based on antenna spin modulation, allowed localizing the source regions in the plasmopause (Décréau et al., 2004) confirming IMAGE observations. CLUSTER tetrahedral configuration of four identical satellites allowed the analysis of specific type of nonthermal continuum. Hence Grimald et al. (2008) showed in the
- 25 nonthermal emissions the presence of spectral peaks organized as several banded emissions with a frequency interval nearby the gyrofrequency at the source. Also details on the wave spectral signature was investigated by El-Lemdani Mazouz et al. (2009) particularly the splitting in fine frequency bands. Another type called 'nonthermal continuum patches' were found to occur within a relatively short time and over a wide frequency range (Grimald et al., 2011). Authors showed that 'patches' events represent 25% of the total nonthermal emissions recorded in one year.
- 30 Physical mechanisms at the origin of the terrestrial nonthermal continuum were first proposed by Frankel (1973) who considered gyro-synchrotron radiation linked to energetic electrons. Gurnett and Frank (1976) made evident correlation between continuum radiation and 1 to 30 keV electrons. Such electrons injection let to intense electrostatic waves nearby the upper hybrid resonance frequency. A linear conversion model was suggested by Jones (1976) where electrostatic waves in the presence of a density gradient would convert into ordinary mode radio waves. In the source region, the density gradient must be
- 35 nearly perpendicular to the magnetic field. This model predicts a beamed radiation outward in two meridional beams at an-



gles of $\gamma = \pm \arctan(f_c/f_p)^{1/2}$ with regard to the magnetic equator. Those angles are depending on f_p the electron plasma frequency and f_c the cyclotron frequency. Also Jones model expects that the generated O-mode emission should be left-hand polarized. The beamed radiation and the O-mode polarization have been confirmed, respectively, by Jones et al. (1987) and Gurnett et al. (1988).

5 In this paper, we analyze the terrestrial non-thermal kilometric radiation observed by ICE/DEMETER experiment in the beginning of the year 2010. The characteristics of this radiation, essentially the spectral features and the spatial occurrence are described in Section 2. Discussion of the outcomes is detailed in Section 3 where principally our results are combined to previous ones. Summary of the main results are given in Section 4.

2 Kilometric radio emission

10 2.1 Overview of HF/ICE observations

We consider in this study the space observations provided by the DEMETER microsatellite. The aim is the analysis of particular spectral features recorded by the ICE experiment in the beginning of the year 2010, i.e. January, February and March. The ICE instrument allows a continuous survey of the electric field over a wide frequency range, from few Hz up to about 3.5 MHz (Berthelier et al., 2006). The electric field component is determined along the axis defined by two sensors. The satellite sun-
15 synchronous half-orbit duration is about 40 min and covering invariant latitude between -65° and $+65^\circ$. The DEMETER satellite orbits are associated to two fixed local times (LTs), at about 10 LT and 22 LT. We use in this investigation the survey mode of the ICE experiment covering the frequency range between few kHz and 3.5 MHz, called hereafter HF-band. The radio wave emissions are alternately recorded on the day- and night-sides of the Earth corresponding respectively to down and up half-orbits. However the main radiations investigated in this paper are observed on the night-side, and rarely on the
20 day-side. Generally the ICE HF-band dynamic spectra allow distinguishing three kinds of spectral emissions depending on the satellite geographical latitudes. The first one is recorded close to the sub-auroral regions at latitudes between 50° and 60° ; it mainly concerns the auroral kilometric radiation described by Boudjada et al. (2009, 2014) and Parrot and Berthelier (2012). The second are mainly ground-based transmitters, low frequency (LF) radiation, appearing at mid-latitudes between 50° and 20° , in both hemispheres (e.g., Parrot et al., 2009; Boudjada et al., 2017).

25 The third kind of emission is a kilometric wave radiation occurring in the vicinity of the equatorial magnetic plane at low latitudes. Hereafter we focus on the analysis of the kilometric radiation in particular the spectral characteristics, the magnetic latitude and the power intensity occurrence. Also the dependence of the power level on the frequency and the magnetic latitude is considered. We use a manually technique which consists to follow and to save with the PC-computer mouse the frequency and the temporal evolution of the terrestrial kilometric radiation. The saved parameters are the observation time (UT hours),
30 the frequency (kHz) and the power level ($\mu V m^{-2} Hz^{-1}$). The collected points are later combined with the satellite orbital parameters like the magnetic latitude and the L-Shell.

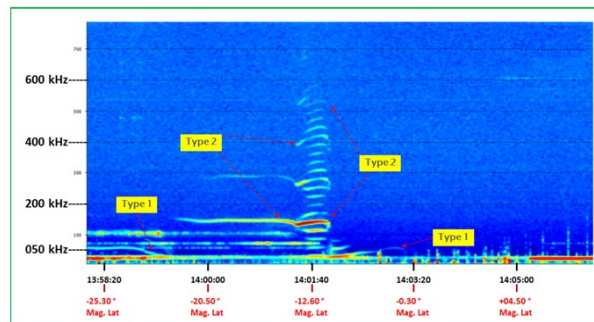


Figure 1. Dynamic spectrum recorded by the ICE/DEMETER experiment where two components, i.e. Types I and II, are indicated. This event was observed on 10th January 2010.

2.2 Frequency and time characteristics

The DEMETER ICE experiment detected terrestrial kilometric emissions in the frequency range between few kilohertz and up to 800 kHz. Fig.1 shows a dynamic spectrum recorded by ICE experiment on 10th January 2010 between 13:58 UT and 14:06 UT. The satellite was on the late evening sector, around 22 LT, at a distance of 665 km. In this time interval the satellite geographical coordinate varied from -18°S to +04°N in latitude and 142° to 138° in longitude. We distinguish two varieties of kilometric emissions as indicated with arrows on Fig.1. The first radiation is called hereafter Type 1, and it appears as a narrow continuum with an instantaneous bandwidth of about 2 kHz at frequencies less than 50 kHz. Type 1 displays negative and positive frequency drifts when the satellite is approaching or leaving the equatorial plane, respectively. Its frequency drift rate is weak and in the order of 0.2 kHz/s. The second emission is called Type 2 and it is composed of parallel narrow-bands, as shown in Fig.1, in a frequency above 50 kHz and up to 800 kHz. The band time duration is, on average, of about 1 minute and decreases to less than one minute when the emission frequency increases. The frequency bandwidth varies from few kHz and up to 20 kHz. Some narrow-bands showed a high power level (red color in Fig.1) when they are compared to other narrow bands. Those enhanced emission bands exhibit an extensive time duration of about 3 minutes.

2.3 Magnetic latitude and power level occurrence

The terrestrial kilometric radiation occurrences in magnetic latitude and power level are shown, respectively, in the top and the bottom panels of Fig.2. The main kilometric emission were recorded when DEMETER was in the southern part of the magnetic equatorial plane. Hence the emissions are detected in the magnetic latitude range between -40° and 20°, as shown in the first panel of Fig.2. We note a clear progressive increase of the kilometric emission occurrence which reaches a maximum at magnetic latitude of -10°. More than 90% of the kilometric radiation occurred in magnetic latitude range between -50° and 0°. Sudden decrease of the occurrence is recorded when the satellite crosses the magnetic equatorial plane. Emission is found

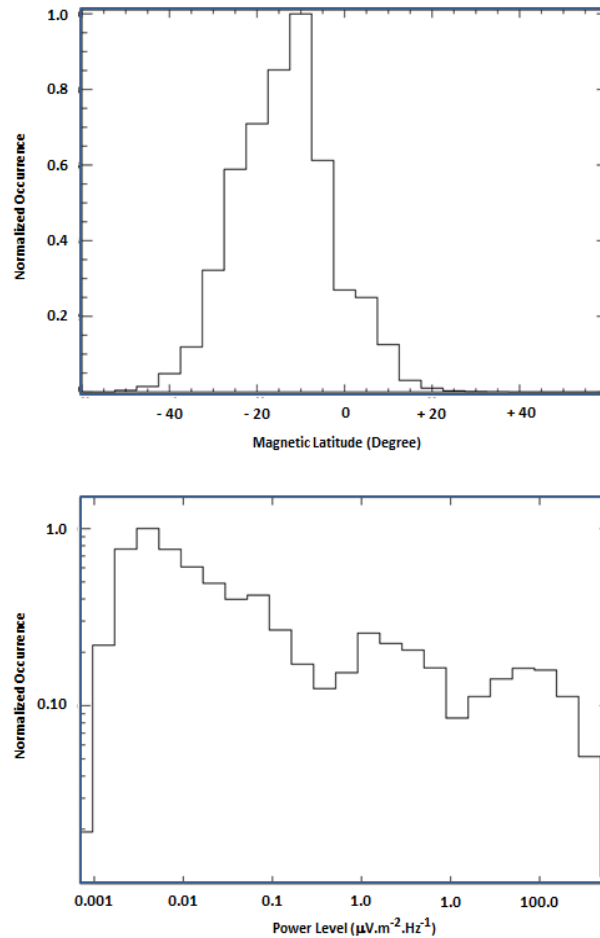


Figure 2. Occurrence of terrestrial kilometric emissions in magnetic latitude (Degree) and in power level ($\mu V m^{-2} Hz^{-1}$).

to be more extended in the southern hemisphere with a clear di-symmetry occurrence before and after the equatorial magnetic plane.

The power level, as displayed in the second panel of Fig.2, is covering a large interval between $10^{-3} \mu V m^{-2} Hz^{-1}$ and $10^{+4} \mu V m^{-2} Hz^{-1}$. More than 70% of the terrestrial emissions have a level less than $1 \mu V m^{-2} Hz^{-1}$ and belong mainly to the southern hemisphere. Above this weak power level, the occurrence of terrestrial kilometric emission is associated to both hemispheres. The intense power level is associated to the kilometric emission occurring mainly at lower frequency, i.e. from few kilohertz and up to 100 kHz (see sub-Section 2.4). We distinguish three occurrence maxima at about $5 \times 10^{-3} \mu V m^{-2} Hz^{-1}$, $1 \mu V m^{-2} Hz^{-1}$ and $80 \mu V m^{-2} Hz^{-1}$. We separate the power level by taking into consideration the interval associated to



the previous maxima. Hereafter green, blue and red colors indicate, respectively, three power level intervals, i.e. $0.001 - 0.7 \mu V m^{-2} Hz^{-1}$, $0.7 - 10 \mu V m^{-2} Hz^{-1}$, and $10 - 10^4 \mu V m^{-2} Hz^{-1}$.

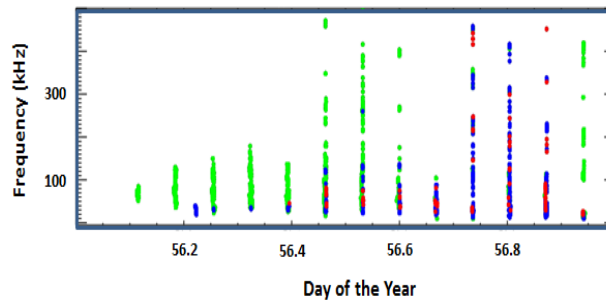


Figure 3. Vertical lines indicate the occurrence of the kilometric emissions observed on 25th Feb. 2010. Those events were recorded on the night-side of the Earth with a time interval of about 01h35mn. Green, blue and red colors specify, respectively, three power level intervals, i.e. $10^{-3} - 0.7 \mu V m^{-2} Hz^{-1}$, $0.7 - 10 \mu V m^{-2} Hz^{-1}$, and $10 - 10^4 \mu V m^{-2} Hz^{-1}$.

Kilometric radio emissions are regularly observed on the night-side (22 LT) before and after the magnetic equatorial plane in the vicinity of the Earth at a distance less than 750 km. Fig.3 displays the daily occurrence of kilometric radio emissions observed by ICE experiment on 25th Feb. 2010. We observe a periodic occurrence of the emission with a time interval of about 1h35 which corresponds to a DEMETER microsatellite full orbit. Each vertical line is considered as an 'event' and corresponds to the recorded emission for a given orbit. The occurrence per day is about 13 events in the optimal case. However from one event to another we note a variation in the frequency bandwidth and also in the power level. The lower part up to 50 kHz is mainly associated to the Type 1, and above this lower frequency limit we distinguish the Type 2 radiation which extended up to 500 kHz, and sometimes more.

2.4 Power level versus frequency and magnetic latitude

Fig.4 displays the power level variation versus the magnetic latitude where the colors indicate different power levels as defined in the previous sub-Section. The weakest intensities (less than $0.7 \mu V m^{-2} Hz^{-1}$) are recorded at magnetic latitudes between -50° and $+30^\circ$ but much more in the southern hemisphere, as displayed in first panel of Fig.4. Structured emissions appear when the magnetic latitude is positive principally after the crossing of the magnetic equatorial plane. One can distinguish five components appearing in four frequency ranges: few kHz - 50 kHz, 70 kHz - 130 kHz, 170 kHz - 250 kHz, 280 kHz - 340 kHz and 380 kHz - 420 kHz. Those radiations are extended in magnetic latitudes in particular at low frequencies around 50 kHz, and decreases at higher frequencies, at about 400 kHz. Terrestrial kilometric emission is quasi-absent between those four frequency bands.

Also structured emissions are observed in the southern part of the magnetic equatorial plane at frequencies above 200 kHz in magnetic latitude between -10° and 0° degrees, as shown in the first panel of Fig.4. Those structures are mainly

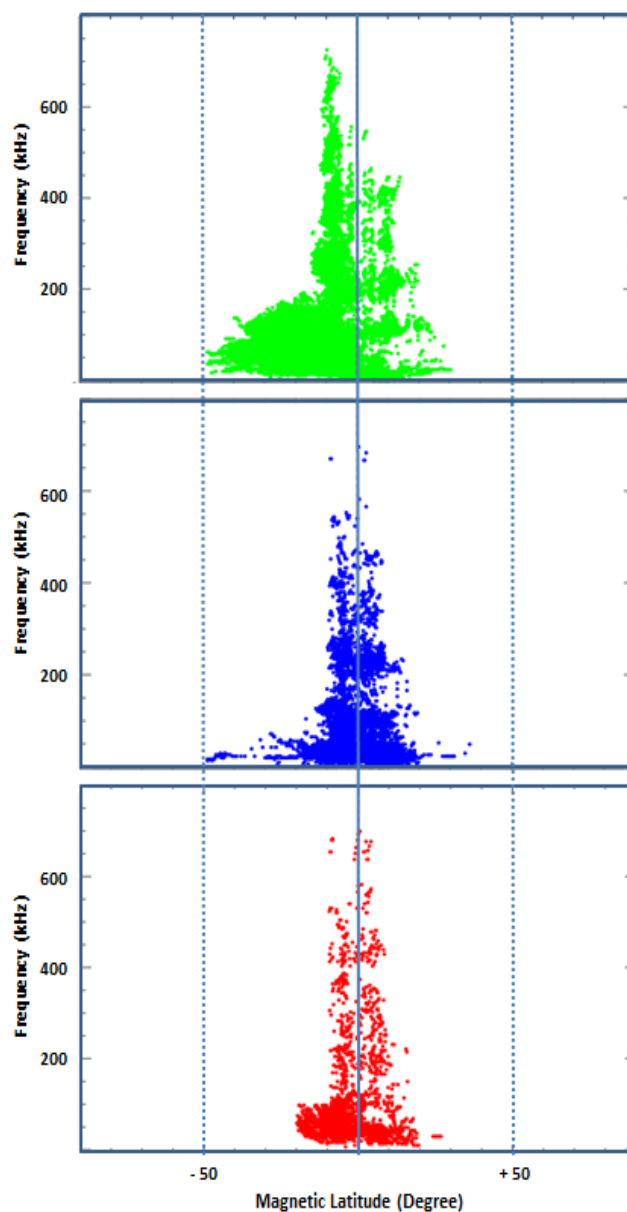


Figure 4. Variation of the power levels versus the frequency (vertical axis) and the magnetic latitude (horizontal axis) for all events. Colors are similar to those used in Fig.3.

extended in frequency, contrary to those observed in northern hemisphere which extended in magnetic latitude. We distinguish four components occurring in the following frequency bands: 200 kHz - 320 kHz, 320 kHz - 450 kHz, 450 kHz - 570 kHz



and 570 kHz - 670 kHz. At frequencies lower than 200 kHz, we note a quasi-absent of structured emission in the southern hemisphere. Terrestrial kilometric emissions continuously occur in magnetic latitude between -50° and 0° . In this interval, we find a positive/negative frequency drift rate of about $+3.75 / -1.25$ kHz/degree when the frequency is higher/smaller than 50 kHz. The terrestrial kilometric emissions is mainly confined to frequencies lower than 150/100 kHz in the southern/northern part of the magnetic equatorial plane when the power level is between 0.7 and $10 \mu V m^{-2} Hz^{-1}$, as displayed in the second panel of Fig.4. Above 150 kHz, the radiations only occur in the frequency bandwidth 180 kHz to about 250 kHz. The power level in the range $10 - 10^4 \mu V m^{-2} Hz^{-1}$ is shown in the third panel of Fig.4. The main terrestrial kilometric emission is nearly symmetrical distributed around the magnetic equatorial plane, between -10° and $+10^\circ$, predominantly above 100 kHz. Below this limit, the radiation covers larger magnitude latitude from -20° to about $+20^\circ$.

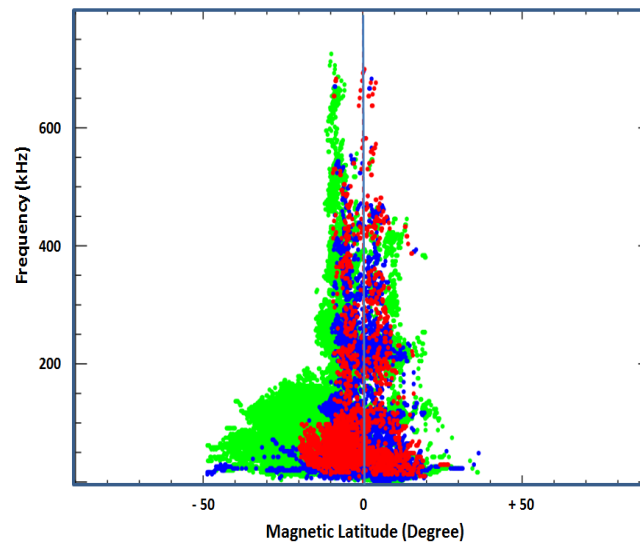


Figure 5. Overlapping of the three power levels displayed in Fig.4. The so-called 'Christmas tree' pattern appears around the magnetic equatorial plane.

10 The overlapping of the three power levels, as shown in Fig.5, allow getting a global shape of the so-called 'Christmas-tree' pattern. We see globally that the kilometric emission is extensively occurring at frequency lower than 150 kHz, and starts to be less confined to the magnetic equatorial plane above this frequency limit. A cut-off appears around 50 kHz which decrease to about few kHz when approaching the magnetic equator plane. This cut-off is characterized by a small frequency drift rate in latitude and a power level in the interval 0.7 and $10 \mu V m^{-2} Hz^{-1}$, i.e. blue color boundary in Fig.5. A second cut-off can be
15 seen when the DEMETER satellite was in the southern hemisphere and absent in northern hemisphere. It starts at latitudes of about -40° and disappears at -18° when the frequency decreases from 150 kHz to 50 kHz. We find that both cut-offs intersected at frequency of about 50 kHz when the magnitude latitude is about -18° .



3 Discussion

We discuss hereafter the kilometric radiation as detected by the DEMETER microsatellite. First we emphasis on the spectral features where we show that similar emissions were recorded by previous satellite at close distance to the Earth but not regularly as allow the DEMETER orbits. Second we discuss the beaming of the kilometric emission taking into consideration its extension in magnetic latitude and its dependence on frequency. Finally, we attempt to localize the source origins where the plasmasphere can be considered as the main location of such emission.

3.1 Spectral features of kilometric emissions

The passage of DEMETER satellite through the magnetic equator allowed re-discovering the terrestrial kilometric radiation. The recorded emissions are similar to those observed by other satellites, like Cluster, GEOTAIL and IMAGE. Hence the two types were also recorded and described in the literature. However the main advantage of DEMETER is its low altitude which was of about 700 km and regular observations of the kilometric emissions. Both components were reported and described as trapped and escaping emissions corresponding, respectively, to Type 1 and Type 2. Of course the spectral features are often comparable and the main alternations may be due to the instrumental time and frequency resolutions, and also the satellite orbits with regard to the source locations. DEMETER recorded emissions on both side of the magnetic equator, and they appear to be more structured in the northern hemisphere. Such frequency patterns may be related to the source regions which should be the plasmasphere. Those lasting bands indicate a 'stable' features in the late evening sector of the plasmasphere, i.e. at about 22 LT.

The parallel narrow bands are mainly associated to the escaping continuum. Green and Boardsen (2006) show a typical example of the kilometric continuum recorded by RPI/IMAGE experiment during a passage of the magnetic equator plane. AKR-X/INTERBALL-1 experiment provided similar emissions particularly in the southern hemisphere at low magnetic latitude and at L-Shell of about 1.2 (Kuril'chik et al., 2001). Observations at fixed frequencies (100 kHz, 252 kHz, 500 kHz and 749 kHz) allowed the analysis of the spectral character of such emissions. Authors showed that the terrestrial kilometric radiation occurrence is depending on the solar activity. Such radiation is regularly recorded during quiet solar activity. Our observations were registered in the begging of the year 2010, nearly eighteen months after the minimum of solar activity, i.e. Aug. 20008.

3.2 Beaming and source locations of kilometric emissions

The power level distribution of the kilometric emission shows restrained and extended deployment around the equatorial magnetic plane. Hence the latitudinal beam is found to be of about 40° when the frequency is, on average, less than 100 kHz. Above this limit and up to about 800 kHz, the latitudinal beam is decreasing and found of about 20° . This general picture is easily seen in the third panel of Fig.4. However we note a clear difference in the beam when the level is less than $1 \mu V m^{-2} Hz^{-1}$, as one can see in the first panel of Fig.4. Hence the terrestrial kilometric beam is different when combing the emission recorded in the southern and northern parts of the magnetic equatorial plane. In the southern one, half of the



Christmas-tree pattern is observed, i.e. beams of 25° and 10° , on average, in the frequency bandwidths 30 kHz-100 kHz and 100 kHz-800 kHz, respectively. On the other side of the equatorial magnetic plane only branches, or limbs, are detected as shown in the first panel of Fig.4. It is evident that emission diagrams are unlike which may be due to combine effects of multi-sources locations and ray path propagations.

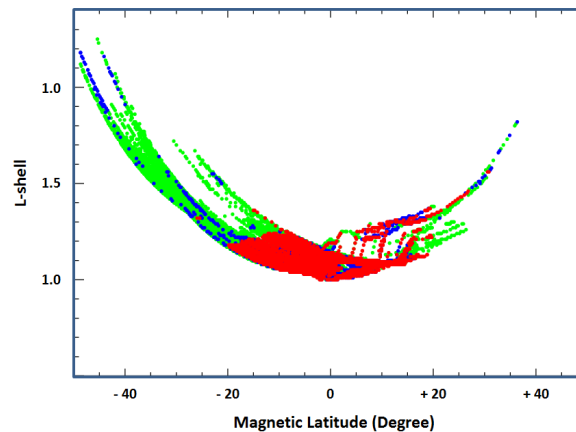


Figure 6. Variation of the terrestrial kilometric emissions versus the L-Shell and the magnetic latitude.

5 The beams of the terrestrial kilometric events are found to depend on the satellite orbits with regard to the magnetic equatorial plane. The two beams associated to the southern hemisphere events are observed in different frequency bandwidth. We may be deal with two source regions localized in the southern part of the magnetic equator but confined to two unlike regions with high and low plasma densities. Fig.6 displays the variation of the L-shell associated to the terrestrial kilometric events versus magnetic latitude of the satellite. The power level is principally found to increase between 1 and 1.4 L-shell when the magnetic
10 latitude of DEMETER is in between -20° and $+20^\circ$. The source locations of terrestrial kilometric radiation seem to be confined to a narrow L-shell region.

Fig.7 provides a sketch of the emission diagrams of the terrestrial kilometric emissions. Those diagrams are different before and after the magnetic equatorial plane. Hollow cones may be considered in the 'southern' source emission with opening angle which is small at frequency of about 700 kHz and increase to 40° around 100 kHz. Multi-beams can be related to
15 the 'northern' sources which looks like a succession of 'laser-beams' emitting at specific frequencies. Southern and northern sources are probably localized in the plasmasphere, as suggested by previous studies (see review of Green et al., 2004). The physical process is depending on the source plasma conditions and the strength of the Earth's magnetic field. Kuril'chik et al. (2001) addressed this physical process by considering the presence of Z and LO escaping modes.

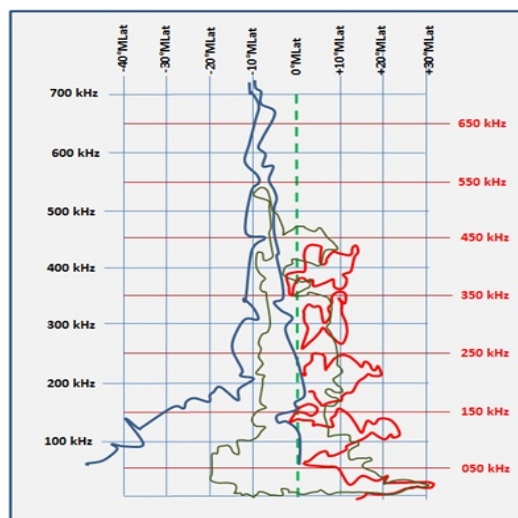


Figure 7. Sketch of the beams observed in the southern (blue color) and the northern (red color) parts of the magnetic equator plane, as resulting from Fig4b. The strong power levels (green-dark color) are recorded at $\pm 10^\circ$ magnetic latitude.

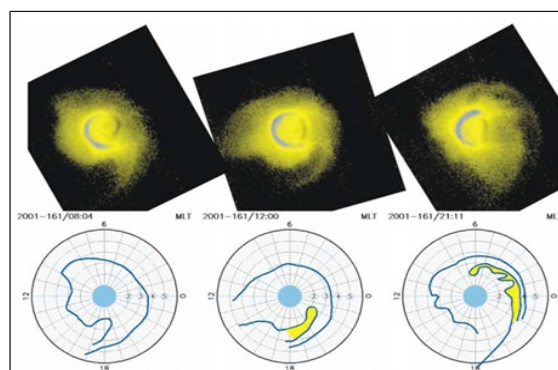


Figure 8. EUV IMAGE observations of the Earth's plasmasphere as reported by Sandel et al (2003). The time evolution of the plume structure is shown with the yellow color.

3.3 Morphological aspects of the plasmasphere

IMAGE scientists reported about density structures recorded by EUV experiment (Burch et al., 2000). Such structures have been discovered by combing IMAGE and Clusters observations. New terms have been defined like channels, crenulations, fingers and shoulders as reviewed in Darrouzet et al. (2009). We consider hereafter the work of Sandel et al. (2003) who



investigated a plasmaspheric event observed on 10th June 2001 using EUV IMAGE observations. The so-called 'Christmas-tree' pattern with different emission diagrams, before and after magnetic equatorial plane, may be compared to the mechanism that can create channel. Fig.8 shows a time evolution of the pre-midnight sector when a drainage plume wrapped around the plasmasphere for the event of 10th June 2001. In the left panel of Fig.8 Sandel et al. (2003) found that the inner part of the plume corotates when the outer parts remain fixed in local time. Four hours later, as seen in the middle panel, the plume starts to wrap around the plasmasphere. After nine hours, the base of the plume has drifted westward in longitude and channel appears between the plume and the main body of the plasmasphere, as displays in the right panel of Fig.8. The DEMETER observations of the terrestrial kilometric emissions provided similar outcomes in particular in the final phase where the channel is generated. We can consider that the plume and the channel are comparable to the kilometric radiation beaming observed before and after the magnetic equatorial plane, respectively. The plume development in the azimuthal plane, as described by EUV IMAGE, has a complement part in the latitudinal plane. In the pre-midnight part of the plasmasphere, the generations of channels, and fingers, may be associated to the 'laser-beams' recorded by DEMETER.

4 Conclusion

We have investigated the terrestrial kilometric radiation recorded by ICE experiment onboard DEMETER satellite. We have distinguished two spectral types which are found to be linked to the 'trapped' and 'escaping' kilometric emission, as previously observed by several satellites. DEMETER orbits allow us to regularly record the terrestrial emission. The occurrence per day is about 13 events in the optimal case. The power level is found in the interval between $10^{-3} \mu V m^{-2} Hz^{-1}$ and $10^{+4} \mu V m^{-2} Hz^{-1}$. The spectral analysis leads to re-construct the so-called 'Christmas-tree' which is the traces of the beaming of the terrestrial kilometric radiation. We have shown that those beams are not similar and depend on the emission frequency and the magnetic latitude. The emission sources are found to be mainly localized in the southern and also in the northern part of the magnetic equator plane. Further analysis allows finding that 'Christmas-tree' pattern may be considered to be related to the EUV temporal evolution of the pre-midnight sector of the plasmasphere where the plume structure ended with the generation of the so-called channel.

Acknowledgements. Acknowledgements. We acknowledge C. N. E. S. for the use of the DEMETER data, and thankful to Jean-Jacques Berthelier who provided us with data from the electric field experiment (Instrument Champ Électrique – ICE).



References

- Berthelier, J.J., Godefroy, M., Leblanc, F., Malingre, M., Menvielle, M., Lagoutte, D., Brochot, J.Y., Colin, F., Elie, F., Legendre, C., Zamora, P., Benoist, D., Chapuis, Y., Artru, J., and Pfaff, R.: ICE, the electric field experiment on DEMETER, *Planet. Space Sci.*, 54, 456–471, 2006.
- 5 Boudjada, M.Y., Biagi, P.F., Al-Haddad, E., Galopeau, P.H.M., Besser, B., Wolbang, D., Prattes, G., Eichelberger, H., Stangl, G., Parrot, M., and Schwingenschuh, K.: Reception conditions of low frequency (LF) transmitter signals onboard DEMETER micro-satellite, *Physics and Chemistry of the Earth*, 102, 70–79, 2017.
- Boudjada, M.Y., Sawas, S., Galopeau, P.H.M., Berthelier, J.J., and Schwingenschuh, K.: Study of AKR hollow pattern characteristics at sub-auroral regions, *European Geosciences General Assembly*, Vienna, 2014.
- 10 Boudjada, M.Y., Galopeau, P.H.M., Berthelier, J.J., Rucker, H.O., Kuril'chik, V.N., and Schwingenschuh, K.: Case studies of terrestrial kilometric and hectometric emissions observed by Demeter/ICE experiment, *European Geosciences General Assembly*, Vienna, 2009.
- Brown, L.W.: The galactic radio spectrum between 130 kHz and 2600 kHz, *Astrophys. J.*, 359–370, 1973.
- Burch, J.L.: IMAGE mission overview, *Space Sci. Rev.*, 91, 1–14, 2000.
- Darrouzet, F., Gallagher, D. L., André, N., Carpenter, D. L., Dandouras, I., Décréau, P. M. E., De Keyser, J., Denton, R. E., Foster, J. C.,
- 15 Goldstein, J., Moldwin, M. B., Reinisch, B. W., Sandel, B. R., and Tu, J.: Plasmaspheric Density Structures and Dynamics: Properties Observed by the CLUSTER and IMAGE Missions, *Space Sci. Rev.*, 145, 55–106, 2009.
- Décréau, P. M. E., Ducoin, C., Le Rouzic, G., Randriamboarison, O., Rauch, J.-L., Trotignon, J.-G., Vallières, X., Canu, P., Darrouzet, F., Gough, M. P., Buckley, A. M., and Carozzi, T.D.: Observation of continuum radiations from the Cluster fleet: first results from direction finding, *Ann. Geophys.*, 22, 2607–2624, 2004.
- 20 Décréau, P.M.E., Fergeau, P., Krasnoselskikh, V., Le Guirriec, E., Lévêque, M., Martin, Ph., Randriamboarison, O., Rauch, J.L., Senée, F. X., Séran, H.C., Trotignon, J.G., Canu, P., Cornilleau, N., de Féraudy, H., Alleyne, H., Yearby, K., Mögensen, P.B., Gustafsson, G., André, M., Gurnett, D.C., Darrouzet, F., Lemaire, J., Harvey, C.C., Travnicek, P., and Whisper experimenters: Early results from the Whisper instrument on Cluster: an overview, *Ann. Geophys.*, 19, 1241–1258, 2001.
- El-Lemdani Mazouz, F., Rauch, J.L., Décréau, P.M.E., Trotignon, J.G., Vallières, X., Darrouzet, F., Canu, P., and Suraud, X., Wave emissions
- 25 at half electron gyroharmonics in the equatorial plasmasphere region: CLUSTER observations and statistics, *Adv. Space Res.*, 43, 253–264, 2009.
- Frankel, M.S.: LF radio noise from the earth's magnetosphere, *Radio Sci.*, 8, 991–1005, 1973.
- Green, J.L., and Boardsen, S.A.: Kilometric continuum radiation, *Radio Sci. Bull.*, 318, 34–41, 2006.
- Green, J.L., Boardsen, S., Fung, S.F., Matsumoto, H., Hashimoto, K., Anderson, R.R., Sandel, B.R., and Reinisch, B.W.: Association of
- 30 kilometric continuum radiation with plasmaspheric structures, *J. Geophys. Res.*, 109, A03203, 2004.
- Grimald, S., El-Lemdani Mazouz, F., Foullon, C., Décréau, P.M.E., Boardsen, S.A., and Vallières, X.: Study of non-thermal continuum patches: wave propagation and plasmopause study, *J. Geophys. Res.*, 116, A07219, 2011.
- Grimald, S., Décréau, P.M.E., Canu, P., Rochel, A., and Vallières, X.: Medium latitude sources of plasmaspheric non thermal continuum radiations observed close to harmonics of the electron gyrofrequency, *J. Geophys. Res.*, 113, A11217, 2008.
- 35 Gurnett, D.A.: The Earth as a radio source: The nonthermal continuum, *J. Geophys. Res.*, 80, 2751–2763, 1975.
- Gurnett, D. A., and Frank, L.A.: Continuum radiation associated with low-energy electrons in the outer radiation zone, *J. Geophys. Res.*, 81, 3875–3885, 1976.



- Gurnett, D. A., and Shaw, R.A.: Electromagnetic radiation trapped in the magnetosphere above the plasma frequency, *J. Geophys. Res.*, 78, 8136-8148, 1973.
- Gurnett, D.A., Calvert, W., Huff, R.L., Jones, D., and Siguira, M.: The polarization of escaping terrestrial continuum radiation, *J. Geophys. Res.*, 93, 12817–12825, 1988.
- 5 Hashimoto, K., Green, J.L., Anderson, R.R., and Matsumoto, H.: Review of kilometric continuum, in *Geospace Electromagnetic Waves and Radiation*, Lect. Not. in Phys., Eds. J. W. LaBelle and R. A. Treumann, Springer, New York, 687, 37–54, 2006.
- Hashimoto, K., Calvert, W., and Matsumoto, H.: Kilometric continuum detected by GEOTAIL, *J. Geophys. Res.*, 104, 28,645- 28,656, 1999.
- Jones, D.: Source of terrestrial nonthermal radiation, *Nature*, 260, 686-689, 1976.
- Jones, D.: Beaming of terrestrial myriametric radiation, *Adv. Space Res.*, 1,373, 1981.
- 10 Jones, D., Calvert, W., Gurnett, D.A., and Huff, R.L.: Observed beaming of terrestrial myriametric radiation, *Nature*, 328, 391, 1987.
- Kuril'chik, V.N., Boudjada, M.Y., Rucker, H.O., and Kopaeva, I.F.: Observations of Electromagnetic Emissions inside the Earth's Plasmasphere from the INTERBALL-1 Satellite, *Cosmic Res.*, 45, 455–460, 2007.
- Kuril'chik, V.N, Boudjada, M.Y, and Rucker, H.O.: The Observations of the Subauroral Nonthermal Radio Emission by AKR-X Receiver onboard of the INTERBALL Satellite, in *Planetary Radio Emissions V*, edited by: Rucker, H.O., Kaiser, M.L., and Leblanc, Y., Austrian Academy of Sciences Press, Vienna, Austria, 202–212, 2001.
- 15 Kurth, W.S., Gurnett, D.A., and Anderson, R.R.: Escaping nonthermal continuum radiation, *J. Geophys. Res.*, 86, 5519–5531, 1981.
- Parrot, M., and Berthelier, J.J.: AKR-like emissions observed at low altitude by the DEMETER satellite, *J. Geophys. Res.*, 117, A10314, 2012.
- Parrot, M., Inan, U.S., Lehtinen, N.G., and Pincon, J.L.: Penetration of lightning MF signals to the upper ionosphere over VLF ground-based transmitters, *J. Geophys. Res.*, 114, A12318, 2009.
- 20 Sandel, B.R., Goldstein, J., Gallagher, D.L., and Spasojevic, M.: Extreme ultraviolet imager observations of the structure and dynamics of the plasmasphere. *Space Sci. Rev.*, 109, 25-46 2003.